MARMARA UNIVERSITY

FACULTY OF ENGINEERING

DESIGN OF AN EJECTOR REFRIGERATION CYCLE AND PERFORMANCE ANALYSIS

Muhammet Ensar TOSUN, Can SOYKAN

GRADUATION PROJECT REPORT

Department of Mechanical Engineering

Supervisor

Assoc. Prof. Dr. Candeniz Seçkin

ISTANBUL, 2022

MARMARA UNIVERSITY

FACULTY OF ENGINEERING

DESIGN OF AN EJECTOR REFRIGERATION CYCLE AND PERFORMANCE ANALYSIS

by

Muhammet Ensar TOSUN,Can SOYKAN

June 15,2022,Istanbul

SUBMITTED TO THE DEPARTMENT OF MECHANICAL ENGINEERING I N PARTIAL FULFILLMENT OF THE REQUIREMENTS FOR THE DEGREE

OF

BACHELOR OF SCIENCE

AT

MARMARA UNIVERSITY

Signature of Author(s) .....Can SOYKAN..... Muhammet Ensar TOSUN.....

Department of Mechanical Engineering

Certified By .....Assoc. Prof. Dr. Candeniz SEÇKİN.....

Project Supervisor, Department of Mechanical Engineering

Accepted By.....Prof.Dr. Bülent EKİCİ.....

Head of the Department of Mechanical Engineering

ACKNOWLEDGEMENT

First of all, we would like to thank my supervisor Assoc. Prof. Dr. Candeniz SEÇKİN, for the valuable guidance and advice on preparing this thesis and giving us moral and material support.

June 15, 2022 Muhammet Ensar TOSUN, Can SOYKAN

CONTENTS

ABSTRACT

Design of an Ejector Refrigeration Cycle and Performance Analysis

In this study, the thermodynamic analysis of an ejector refrigeration cycle is presented. The most important aspects of the operation and performance of the ejector refrigeration cycles are discussed. Based on the mathematical model, a simulation program is developed to analyse the physical mechanism of the cycle. The results of the applied mathematical model and the developed simulation program are reported. Refrigerant (R134a) is investigated by varying the ratio of primary nozzle exit area to throat area, condenser pressure and heat exchanger pressure to determine the effects on system performance. According to the results within the specified ranges, the COP and cooling capacity are inversely proportional to the condenser pressure and the ratio of primary nozzle exit area to throat area. On the other hand, the COP and cooling capacity are directly proportional to the heat exchanger pressure.

SYMBOLS

A : cross-sectional area (m2)

C : speed of sound (m/s)

h : specific enthalpy (kJ/kg)

$\dot{m}$: mass flow rate (kg/s)

P : pressure (kPa)

q : quality

$\dot{Q}$: rate of heat transfer (kW)

s : specific entropy (kJ/kg K)

T : temperature (°C)

V : velocity (m/s)

v : specific volume (m^3 /kg)

w : entrainment ratio

$\dot{W}$: power (kW)

x : concentration

η : efficiency

ρ : density

1,2,.. : number of state-points in Fig. 2.1. and Fig. 2.2.

SUBSCRIPTS

a : mixed flow/cross section a in Fig. 2.2.

b : shocked flow/cross section b in Fig. 2.2.

cond : condenser

evap : evaporator

in : input in the heat exchanger

is : isentropic

m : primary nozzle exit

mass : mass transfer

net : net

p : pump

Q : heat transfer

ref : refrigeration

s : secondary nozzle exit

tot : total

ABBREVIATIONS

COP : Coefficient of Performance

ERC : Ejector Refrigeration Cycle

HE : Heat Exchanger

LIST OF FIGURES

PAGE

LIST OF TABLES

PAGE

1-INTRODUCTION

Worldwide energy demand have increased rapidly since the industrial revolution. Hence, amount of produced energy has showed a parallel pattern. Oil is the most used fuel of energy generation plants (with the share of 33.1%), followed by coal with 30.3% and natural gas (23.7%) [1]. As a result, approximately 90% of the average energy need is supplied by using fossil fuels. By far, the most of the CO_2 emission from energy generation processes is originated by coal burning. Oil is the second which causes one third of CO_2 emission caused by coal burning. On the other hand, natural gas is in the third place emits half of CO_2 emitted by oil combustion [2]. Nowadays, air pollution which is caused by use of fossil fuels causes approximately 5 million premature deaths each year all over the World [3]. In U.S, the electricity generation capacity of natural gas power plants has been increased 150% since 2002. On the other hand electricity generation capacity coal fired power plants have decreased nearly by 20% [4]. Combined cycles recovers the rejected heat from one sub-cycle and generates some additional system outputs (such as cooling, heating, extra power, etc.). Due to the utilization of the rejected heat, plants use its fuel (and hence, natural energy sources) more efficiently. Efficiency of the natural gas fired combined power plants between 45% - 57% [5].

In 2000, a combined power and refrigeration cycle was proposed by Feng et al. was suggesting that the separated rich ammonia-water mixture enters to the condenser and becomes liquid. Then it enters to the super heater its temperature increases. After it enters the turbine and generates power by expanding. Due to the expansion its temperature decreases. Finally, that cold working fluid enters the evaporator and turns into gas and creates cooling effect [6]. In 2009, Wang et al. proposed a development to the cycle proposed by Feng et al., an ejector placed between separator and condenser. When an ejector is placed, the separated rich vapor enters the ejector and draws in the low pressured rich vapor which comes out from the evaporator. By the ejector, the amount of the refrigerant entering to the condenser and evaporator is increased because when the cycle does not have an ejector, the refrigerant is only supplied by separator. But when an ejector is added, apart from the refrigerant coming from the separator, an additional amount of refrigerant comes from the evaporator. So, when the cycle with ejector and without ejector is compared, the cycle that ejector is used has 9.5% more cooling capacity [7].

Sun et al. proposed a combined cycle that consists of ERC (Ejector refrigeration cycle) and Organic Rankine Cycle. In that cycle, working fluid which is R113 leaves the turbine after power generation and enters into the ejector as primary flow (at higher temperature compared to the fluid coming from the evaporator) and it entrains the working fluid coming from the evaporator of the refrigeration cycle. Then the entrained and mixed flow enters the condenser of the refrigeration cycle. At the exit of the condenser, the flow splits into two parts: one part goes to the evaporator in order to generate power, other part goes to the second evaporator to perform cooling. In order to get efficient cooling performance, the waste heat temperature should be within the limits of 140-220 °C [8].

ERC's (Ejector refrigeration cycle) are more performant than traditional cycles. In addition, ERCs can use waste heat. It increases energy efficiency by using waste heat from many power plants. Increasing the efficiency of these power plants, which are already damaging the environment, is needed to reduce both the economic and environmental damage [9]. Ejector refrigeration cycles use the ejector instead of the compressor in the cycle with no additional energy consumption. Therefore it is likely to observe significant amount of energy saving by replacing ejector with compressor. Another important advantage of an ejector refrigeration cycle compared to other refrigeration cycles is that there are no moving parts. The absence of moving parts makes the system simpler. This simplicity also provides reliability and low cost of maintenance [10]. The first study on the ejector refrigeration cycle was done by Sun in 1996. This work was done theoretically and calculations were made by considering three different refrigerants which are R152a, R134a and R123. Among these three refrigerants, the highest COP is obtained for R152a (23.5 %) [11]. In the following years, COP values obtained in theoretical studies increased. In 2004, Selvaraju and Mani obtained COP of 48% using R134a in their calculations. Two years later, the same authors obtained the COP of 27% in their experimental study [12]. These studies show that there is a data inconsistency between theoretical and experimental studies.

Parametric analysis of different ERC have been presented so far. It is seen that there is an optimum area ratio (primary nozzle exit area divided by throat area) to achieve maximum COP and cooling capacity and this ratio is pressure specific [13]. That is why this ratio is examined as one of the parameters in this study.

In this study, thermodynamic analysis of an ERC is presented. The effect of system operational parameters (heat exchanger pressure, condenser pressure, ratio of primary nozzle exit area to throat area) on refrigeration cycle COP and cooling performance is investigated.

2. DESCRIPTION OF THE SYSTEM

In this study an ejector refrigeration cycle is thermodynamically analysed. Components of the ERC can be listed as; heat exchanger, ejector, condenser, valve, evaporator and pump. The heat energy that obtained by the heat exchanger is transferred to the refrigerant. As a result of that transfer, the phase of the refrigerant is changed to saturated vapor at the exit of the heat exchanger. Vapor is at high temperature and pressure at the exit of HE.

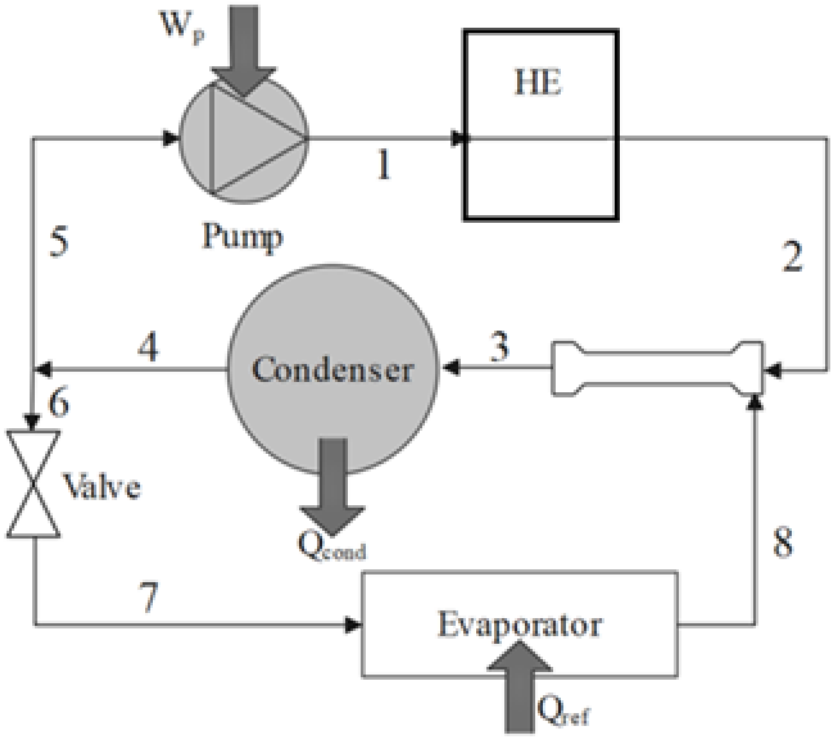

Fig. 2.1. Schematic Overview of the Ejector Refrigeration Cycle (ERC)

As shown in the Fig. 2.1, the vapor which is named as motive flow, enters to the primary nozzle of the ejector. Then the motive flow entrains the refrigerant that exits from the evaporator. Entrained flow is saturated vapor and it is called as secondary flow. Inside the ejector motive and secondary flows mix. Detailed explanation about the mixing process and working principle of the ejector will be done further. At the exit of the ejector the pressure of the refrigerant has a value between the pressures of heat exchanger and evaporator. Mixed flow enters to the condenser and the mixture rejects heat. Therefore it turns into saturated liquid at the exit of the condenser. After leaving the condenser the mixture splits into two streams. One part of the flow enters to pump and pumped to the heat exchanger. Other part of the flow enters to the expansion valve. The pressure of the refrigerant decreases then that refrigerant enters to the evaporator and change its phase to the saturated vapor by absorbing heat from the environment. Thus cooling operation is performed. As it was mentioned earlier, the vapor that left from the evaporator is vacuumed by the motive flow and that completes the cycle.

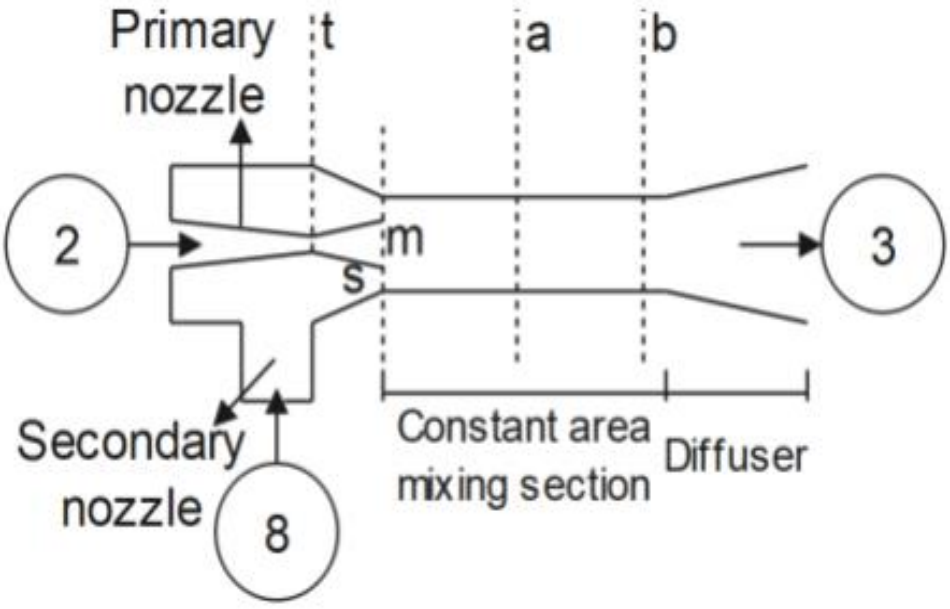

Fig. 2.2. Schematic Representation of Ejector Design

Ejectors can be divided into 2 groups regarding to mixing process of primary and secondary flow. First type is called constant area mixing ejectors. In this type of ejectors the exit of the primary nozzle is placed inside the suction chamber. Therefore the mixing occurred

at the suction chamber while pressure is constant. However, in the other type of the ejectors, namely “constant area mixing ejectors”, the exit of the nozzle is placed at the inlet of the constant area section of the ejector. Mixing occurs in the constant area mixing section. For constant pressure mixing ejectors, it was found that if the distance between the nozzle exit and inlet of the constant area section divided to the diameter of the constant area mixing section is equal to 1.5 [14], the ejector will work at its maximum performance. When constant area mixing ejectors are considered, performance maximization alternatives are relatively less compared to constant pressure mixing ejectors. Nevertheless its performance can be increased by optimizing the area ratio. In the earlier studies, performance of constant pressure ejectors is higher than the other type of ejector [15]. However, it is stated that it is not possible to create a theoretical approximation that decreases the error between theoretical and experimental results for the constant pressure mixing ejectors [16]. For this reason in that study, constant are mixing ejector is used in ERC design.

Fig. (2.2) represents the constant area mixing ejector. Letters t,s,m,a and b in the Fig (2.2) are indicating the critical cross sections. The motive flow enters to the primary nozzle and passes through the convergent-divergent nozzle. While the flow is passing inside the nozzle, its speed continuously increases and at the cross section t it reaches speed of sound so flow chokes. In other words, the flow transforms subsonic to supersonic at that cross section. Refrigerant expands at cross section m in Fig. (2.2) therefore its pressure decreases. It is known that at the supersonic flow, when cross sectional area increases the velocity of the fluid will increase. Therefore, while the fluid expands its speed continues to increase. At the cross section m in Fig. (2.2), pressure of the refrigerant is less than the evaporator pressure. That pressure difference creates a localized low pressure region. At that region, motive fluid vacuums (draws in) the vapor that left the evaporator, also called as secondary flow. While the secondary flow is moving inside the nozzle its speed will increase and at the cross section s in Fig. (2.2), it expands. After both flows expand into the constant area mixing section, mixing starts. It was assumed that the mixing will be occurred at constant pressure. In the cross section a in Fig. (2.2), the mixing completes. Shock wave forms while the mixture is passing through cross section b in Fig. (2.2). Due to the shock, pressure rapidly increases and velocity decreases. After passing the cross section b in Fig. (2.2), the flow reaches the diffuser of the ejector so it expands and its pressure increases and velocity decreases once more. The pressure of the mixture while it is leaving the ejector is equal to condenser pressure.

2.1. Assumptions for Mathematical Model and Computational Programming

The assumptions applied in the ERC analysis are listed below [17,18,19,20].

- Steady-state, one-dimensional, frictionless flow.
- The potential energy and kinetic energy changes in the devices are neglected.
- Working fluid leakage is neglected.
- Head loss in pipes and other components are neglected.
- Heat losses to the environment from all components and pipes (except the condenser) are neglected.
- Throttling process in the valve is isenthalpic.
- Losses in the pump and ejector are accounted for by means of isentropic efficiencies.

Below assumptions are made to perform the mathematical model of ERC [17,21,22].

- The motive and secondary flows at the ejector inlet and also at the exit of the ejector, velocity of the refrigerant is zero.
- The design pressure at the primary nozzle exit is uniform and the secondary flow reaches critical conditions at this level [18,23]
- During critical-mode operation in the ejector, both flows are chocked and the entrainment is constant.
- At the exit of the condenser, the refrigerant is at saturated liquid state.
- At the ejector inlet, both flows are at saturator vapor state.
- Temperature and pressure are constant through the evaporator and the condenser.

In this study, a simulation application which is named Engineering Equation Solver (EES) was used to determine how the ejector refrigeration cycle gives results in different conditions. All the features of the refrigerants are available in the EES application and simulation has been made using these features. The conservation of mass, energy and momentum principles are successively applied to each element of the analysed cycle in the

mathematical model of the performed thermodynamic analysis. Mathematical formulas used in the thermodynamic modeling of ERC are reported below.

2.2. ERC Modeling

In this section, the formulas required for the simulation of ERC system are given. Some data are entered as input in the simulation program. These inputs are; condenser pressure (P_{cond}), evaporator pressure (P_{evap}), heat exchanger pressure (P_{HE}), total mass flow rate of the refrigerant ($\dot{m}_{tot}$), isentropic efficiency of the pump(η_p), primary nozzle (η_m), secondary nozzle (η_s), diffuser (η_d), cross-sectional area of the primary nozzle exit (A_m).

The entrainment ratio (w) is calculated as the ratio of the low pressure steam secondary flow mass flow rate ($\dot{m}_8$) to the motive ($\dot{m}_2$) flow mass flow rate.

$$w = \frac{\dot{m}_8}{\dot{m}_2} \tag{2.1}$$

The following equations were obtained based on the above assumptions.

$$P_{HE} = P_1 = P_2 \tag{2.2}$$

$$P_{cond} = P_3 = P_4 = P_5 = P_6 \tag{2.3}$$

$$P_{evap} = P_7 = P_8 \tag{2.4}$$

$$q_2 = q_8 = 1 \tag{2.5}$$

$$q_4 = q_5 = q_6 = 0 \tag{2.6}$$

$$\dot{m}_{tot} = \dot{m}_3 = \dot{m}_4 \tag{2.7}$$

$$\dot{m}_1 = \dot{m}_2 = \dot{m}_5 \tag{2.8}$$

$$\dot{m}_6 = \dot{m}_7 = \dot{m}_8 \tag{2.9}$$

In above equations, P, q and $\dot{m}$ are pressure, quality and mass flow rate of the refrigerant at subscripted state-points, respectively.

Specific enthalpy of the motive flow at the primary nozzle exit (h_m) is determined by following equations:

$$\eta_m = \frac{h_2 - h_m}{h_2 - h_{m,is}} \tag{2.10}$$

Where $h_{m,is}$ is the specific enthalpy of the motive flow at the end of the isentropic expansion process in the primary nozzle, h and s are the specific enthalpy and specific entropy of the refrigerant at subscripted state-points in Figure 2.1 and Figure 2.2.

Velocity of the motive flow at the primary nozzle exit (V_m) is determined by the following equation:

$$V_m = \sqrt{2(h_2 - h_m)} \tag{2.11}$$

According to the mass conversation equation, following equation must be satisfied at the primary nozzle outlet.

$$\dot{m}_2 = \dot{m}_m = \left(\frac{1}{1+w}\right)\dot{m}_{tot} = \frac{V_m A_m}{v_m} \tag{2.12}$$

Where $\dot{m}_{total}$ is the total mass flow rate of the refrigerant ($\dot{m}_2 + \dot{m}_8$), v_m is the specific volume of the refrigerant at the primary nozzle exit.

Secondary flow's specific enthalpy h_s is determined by the following equations:

$$\eta_s = \frac{h_8 - h_s}{h_8 - h_{s,is}} \tag{2.13}$$

Where $h_{s,is}$ is the specific enthalpy of the secondary flow at the end of the isentropic expansion process in the secondary nozzle, P_s is the secondary flow's pressure, h and s are the specific enthalpy and specific entropy of the refrigerant at subscripted state-points in Figure 2.1 and Figure 2.2.

$$V_s = \sqrt{2(h_8 - h_s)} \tag{2.14}$$

$$\dot{m}_8 = \dot{m}_s = \left(\frac{1}{1+w}\right)\dot{m}_{tot} = \frac{V_s A_s}{v_s} \tag{2.15}$$

Where C_s the sound is speed at section s, at the secondary nozzle exit A_s and v_s are the cross-sectional area and the specific volume of the refrigerant, respectively.

A constant area and constant pressure is assumed at the time of mixing. The primary and secondary flows retain their identity a short distance before the exit of their respective nozzles, before mixing takes place in cross-section a in Figure 2.2. According to the mass, momentum

and energy conservation equations, the enthalpy and velocity of the mixed fluid can be calculated using the following equations:

$$A_a = (A_m + A_s) \tag{2.16}$$

$$\dot{m}_a = \dot{m}_m + \dot{m}_s = \dot{m}_{tot} \tag{2.17}$$

Conservation of momentum equation:

$$P_a A_a + \dot{m}_{tot} V_a = \varphi(P_m A_m + \dot{m}_m V_m + P_s A_s + \dot{m}_s V_s)$$

$$= P_a A_a + \frac{A_a V_a^2}{v_a} = \varphi(P_m A_m + \frac{A_m V_m^2}{v_m} + P_s A_s + \frac{A_s V_s^2}{v_s}) \tag{2.18}$$

Where P_a is the pressure of the mixed flow before shock, A_a is the cross-sectional area at cross-section a, φ is the coefficient of frictional loss. [24]

Conservation of mass equation:

$$\dot{m}_{tot} = \frac{V_a A_a}{v_a} \tag{2.19}$$

V_a and v_a are velocity and specific volume of the refrigerant at cross-section a in Figure 2.2.

h_a which is specific enthalpy at cross-section a can be calculated using the following equations:

$$\dot{m}_{tot} \left[h_a + \frac{V_a^2}{2}\right] = \dot{m}_m \left[h_m + \frac{V_m^2}{2}\right] = \dot{m}_s \left[h_s + \frac{V_s^2}{2}\right] \tag{2.20}$$

Eq. (30) must be satisfied.

In section b at Fig. 2.2, shock occurs. The most common and realistic position, according to Lear et al. [25] , is the appearance of a normal shock wave in the constant area mixing section, resulting in subsonic flow after the shock. Rankine-Hugoniot equations are used for thermodynamic magnitudes after the shock wave [26, 27].

$$\frac{P_b}{P_a} = \frac{2kM_a^2 - (k-1)}{k+1} \tag{2.21}$$

$$\frac{\rho_b}{\rho_a} = \frac{v_a}{v_b} = \frac{(k+1)M_a^2}{(k-1)M_a^2 + 2} \tag{2.22}$$

Here, k is the ratio of specific heats $(\frac{c_p}{c_v})$, c_p and c_v are specific heats at constant pressure and constant volume, respectively. ρ_a and ρ_b are density at section a and b, respectively. M_a is the Mach number at cross-section a.

h_3 which is specific enthalpy at the diffuser exit can be determined by using conservation of energy:

$$\dot{m}_{tot}h_3 = \dot{m}_2h_2 + \dot{m}_sh_8 \tag{2.23}$$

The actual enthalpy at the diffuser outlet can also be determined as:

$$\eta_d = \frac{h_{3,is}-h_b}{h_3-h_b} \tag{2.24}$$

η_d is the diffuser isentropic efficiency, $h_{3,is}$ is the specific enthalpy at the end of the isentropic process in the diffuser, P_3 is the pressure at the exit of the diffuser and s_b is the specific entropy at the diffuser inlet.

Next, to find the rate of heat rejection from condenser ($\dot{Q}_{cond}$), rate of heat input ($\dot{Q}_{in}$), power requirement of pump ($\dot{W}_p$) and rate of heat absorption thruoug the evaporator (In other name, refrigeration capacity) ($\dot{Q}_{ref}$) below presented procedure is applied.

$$\dot{Q}_{cond} = \dot{m}_{tot}(h_3 - h_4) \tag{2.25}$$

$$\dot{W}_p = \frac{v_5(P_1-P_5)}{\eta_p}\dot{m}_1 \tag{2.26}$$

$$\dot{W}_p = \dot{m}_1(h_1 - h_5) \tag{2.27}$$

$$\dot{Q}_{in} = \dot{m}_1(h_2 - h_1) \tag{2.28}$$

$$h_6 = h_7 \tag{2.29}$$

$$\dot{Q}_{ref} = \dot{m}_7(h_8 - h_7) \tag{2.30}$$

$$COP = \frac{\dot{Q}_{ref}}{\dot{Q}_{in}} \tag{2.31}$$

3. RESULTS AND DISCUSSION

Thermodynamic analysis for ERC was performed by implementing the mathematical model of ERC into a simulation software. Effects of primary nozzle area ratio [$\frac{A_m}{A_t}$], condenser pressure (P_{cond}), heat exchanger pressure (P_{HE}), on the refrigeration capacity and COP are investigated while other parameters are kept constant. Operational parameters of ERC are listed in Table 3.1.

Table 3.1. Operational Parameters and Boundary Conditions of ERC Simulation Program

Isentropic efficiency of the pump - η_p (%)	80
Isentropic efficiency of the ejector parts - η_m, η_s, η_d (%)	90
Condenser pressure - P_{cond} (kPa)	850
Evaporator pressure - P_{evap} (kPa)	415
Heat exchanger pressure - P_{HE} (kPA)	2635
Total mass flow rate of the refrigerant - $\dot{m}_{tot}$ (kg/s)	4

In this study, thermodynamic analysis is performed for an ERC in which R134a is the working fluid. Variation of COP and $\dot{Q}_{ref}$ with $\left[\frac{A_m}{A_t}\right]$ ratio is shown in the Fig.3.1. As the ratio increase, $\dot{Q}_{ref}$ and COP decrease. It is observed that pressure at the section m increases as the ratio gets higher (Fig.3.1). As a result, pressure difference between the evaporator exit and cross-section m declines. Therefore the amount of the refrigerant drawn from the evaporator decreases. Based on Eq. (2.30), $\dot{Q}_{ref}$ is proportional to the $\dot{m}_7$ and therefore $\dot{Q}_{ref}$ also decreases with increasing $\left[\frac{A_m}{A_t}\right]$ ratio. Since the total mass flow rate of working fluid through the system is constant, the amount of the refrigerant enters to the HE increases. Based on the Eq. (2.28), $\dot{Q}_{in}$ also increases. Based on the Eq. (2.31), decreasing $\dot{Q}_{ref}$ and increasing $\dot{Q}_{in}$ result in a drop in COP of ERC system.

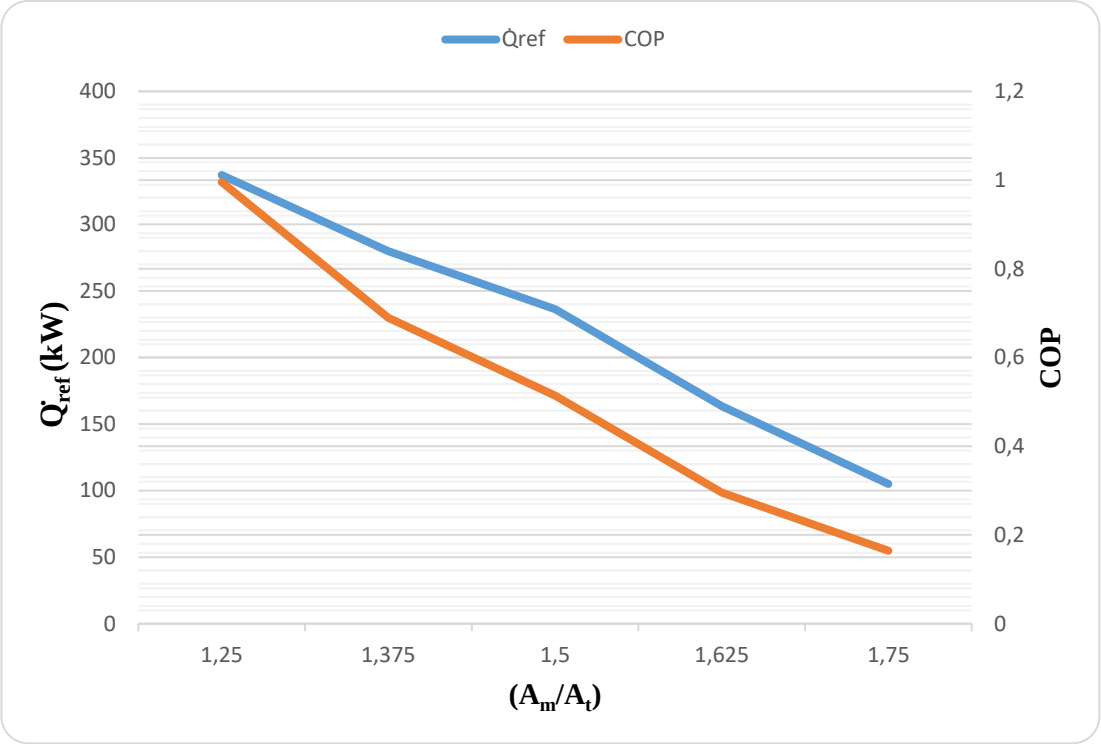

Fig. 3.1. COP and $\dot{Q}_{ref}$ of ERC at different $\frac{A_m}{A_t}$ ratio

From the Fig. 3.2, variation of COP and $\dot{Q}_{ref}$ with respect to P_{cond} is represented. It is seen that when P_{cond} gets higher, COP and $\dot{Q}_{ref}$ decrease. From the outputs of the simulation, it is seen that as P_{cond} increases, enthalpy of the refrigerant at the exit of the condenser also increase since the enthalpy of working fluid at the condenser exit rises with growing pressure of the condenser. The pressure of the evaporator is kept constant as stated earlier. Therefore the enthalpy at the exit of the evaporator remains the same. On the other hand, enthalpy of the refrigerant entering to the evaporator increases with growing P_{cond} due to the isenthalpic process in the valve. Hence, enthalpy difference between the exit and inlet of the evaporator drops which causes a decline in $\dot{Q}_{ref}$, based on Eq. (2.30). Added to this, $\dot{m}_1$ rises with increasing P_{cond}. As a result, based on Eq. (2.28), it can be seen that $\dot{Q}_{in}$ rises, with increasing P_{cond}. By considering Eq. (2.31), it is obvious that COP and $\dot{Q}_{in}$ are inversely proportional. Therefore due to the decreasing $\dot{Q}_{ref}$ and increasing $\dot{Q}_{in}$, COP drops in Fig. 3.2.

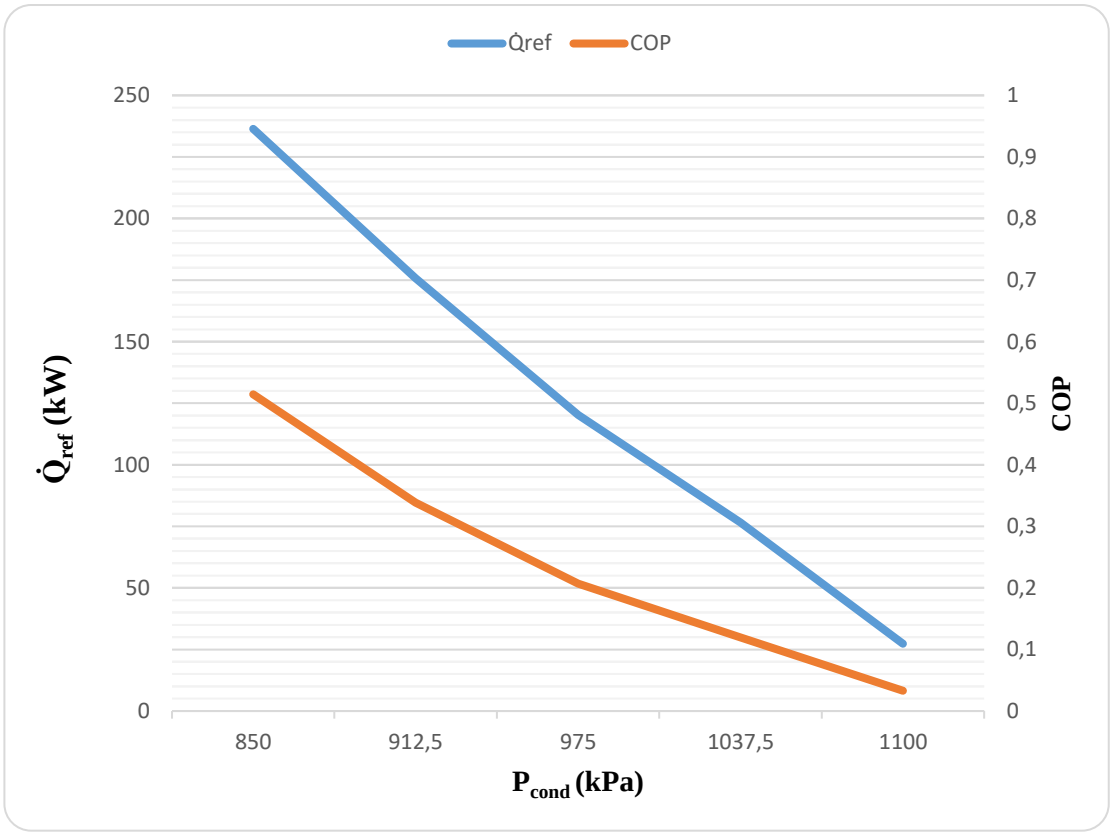

Fig. 3.2. COP and $\dot{Q}_{ref}$ of ERC at Different Condenser Pressures (P_{cond})

In Fig 3.3, COP of ERC at different heat exchanger pressures (P_{HE}) is presented. COP of ERC is increasing with increasing P_{HE} as seen in Fig. 3.3. It is observed that increase of P_{HE} results a rise in both $\dot{Q}_{ref}$ and COP. The outputs of simulation shows that while P_{HE} is increasing, mass flow rate of the refrigerant passing from the evaporator ($\dot{m}_7$) also increases. When Eq. (2.30) is considered, an increment in mass flow rate of the refrigerant passing from the evaporator causes a rise in $\dot{Q}_{ref}$. The total mass flow rate ($\dot{m}_{tot}$) is constant, i.e., mass flow rate of the refrigerant passing through the HE is decreasing with increasing P_{HE} .This leads a decline in $\dot{Q}_{in}$, based on Eq. (2.31). Decreasing $\dot{Q}_{in}$ and increasing $\dot{Q}_{ref}$ yield the reduction of COP (as seen in Fig 3.3.) with increasing P_{HE}.

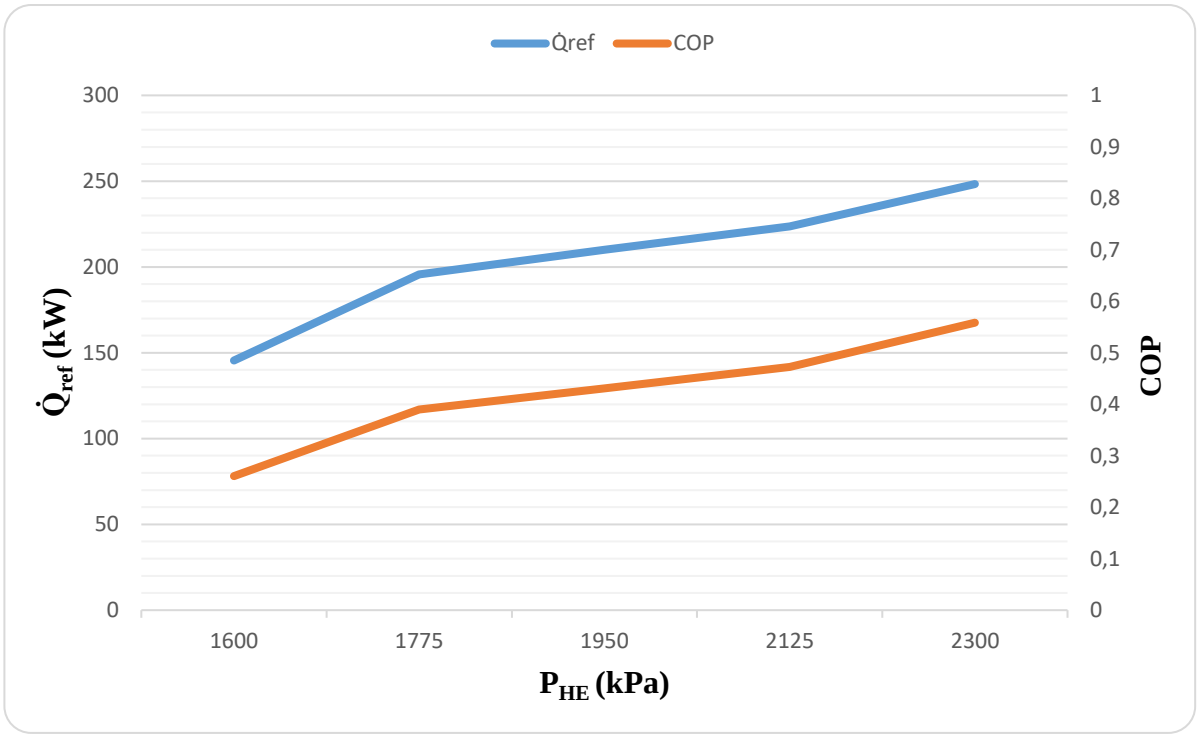

Fig. 3.3. COP and $\dot{Q}_{ref}$ of ERC at Different Heat Exchanger Pressures (P_{HE})

4. CONCLUSION

Thermodynamic analysis of ejector refrigeration cycle is performed in this study. Also the effects of three key parameters which are related to ejector design (Fig. 2.2) and two operational parameters of the cycle (Table 3.1) are investigated. In order to perform this study, a mathematical model is built and the model is implemented into a simulation software. By utilizing the mathematical model and the simulation software, the effects of three parameters listed below are investigated.

First, the behaviour of cooling capacity ($\dot{Q}_{ref}$) and COP were investigated while the ratio of primary nozzle exit area to throat area ($\frac{A_m}{A_t}$) varies. Regarding the outputs, it can be reported that the design of the convergent nozzle has a strong influence on both refrigeration capacity and COP. When the area ratio is adjusted to 1.75 from 1.25, 69% reduction in refrigeration capacity and 83% reduction in COP are observed.

Secondly, the behaviour of cooling capacity ($\dot{Q}_{ref}$) and COP are investigated while the condenser pressure (P_{cond}) increases. Within the interval of 850-1100 kPa of condenser pressure, the refrigeration capacity decreased to 27.33 kW from 236.4 kW which means nearly 88% fall. Also COP is decreased by 94%. Therefore, under the given operating conditions (Table 3.1), rise of condenser pressure yields a substantial increase in COP and $\dot{Q}_{ref}$.

The last parameter is the heat exchanger pressure (P_{HE}). Variation of the refrigeration capacity and COP at increasing heat exchanger pressure is investigated. When the heat exchanger pressure is 1600 kPa, $\dot{Q}_{ref}$ is 145.5 kW. After adjusting the pressure to 2300 kPa, $\dot{Q}_{ref}$ increases to 248.3 kW. This means 70% rise in the refrigeration capacity. Also an increment of COP is observed. Increasing the pressure to 2300 kPa results 115% increase in COP. Therefore, similar to condenser pressure, the heat exchanger pressure increase also has a significant effect on COP and $\dot{Q}_{ref}$.

As a result, change in condenser and heat exchanger pressure affects the performance of the cycle significantly. The effect of these two parameters might be expected. However, this study shows that the ejector design is also an important factor for the performance of the cycle. This study reports that dimensional specifications of the convergent divergent nozzle should be determined studiously.

REFERENCES

[1] BP Statistical Review of World Energy, 2012. British Petroleum (BP), London, UK.

[2] Bölük, G., Mert, M., (2015). The renewable energy, growth and environmental Kuznets curve in Turkey: An ARDL approach, Renewable and Sustainable Energy Reviews, Volume 52, Pages 587-595.

[3] Amini, H., et al., (2019). Short-term associations between daily mortality and ambient particulate matter, nitrogen dioxide, and the air quality index in a Middle Eastern megacity. Environmental Pollution, Volume 254, Part B.

[4] U.S. Energy Information Administration, Annual Electric Generator Report,(2019).

[5] Storm, K., (2020). Industrial Construction Estimating Manual, Chapter 6 - Combined cycle power plant (1×1) labor estimate, Pages 95-159.

[6] Xu, F., Goswami, D. Y., & Bhagwat, S. S. (2000). A combined power/cooling cycle. Energy, 25(3), 233-246.

[7] Wang, J., Dai, Y., Zhang, T., & Ma, S. (2009). Parametric analysis for a new combined power and ejector–absorption refrigeration cycle. Energy, 34(10), 1587-1593.

[8] Sun, W., Yue, X., & Wang, Y. (2017). Exergy efficiency analysis of ORC (Organic Rankine Cycle) and ORC-based combined cycles driven by low-temperature waste heat. Energy Conversion and Management, 135, 63-73.

[9] Kasaeian, A., Shamaeizadeh, A., & Jamjoo, B. (2022). Combinations of Rankine with Ejector Refrigeration Cycles: Recent Progresses and Outlook. Applied Thermal Engineering, 118382.

[10] Yu, M., & Yu, J. (2021). Thermodynamic analyses of a flash separation ejector refrigeration cycle with zeotropic mixture for cooling applications. Energy Conversion and Management, 229, 113755.

[11] Sun DW. Comparative study of the performance of an ejector refrigeration cycle operating with various refrigerants. Energy Conversion and Management. 1999, 40:873-84.

[12] Selvaraju A, Mani A. Analysis of an ejector with environment friendly refrigerants. Appl. Therm. Eng. 2004, 24:827-38.

[13] Yapıcı, R., Ersoy, H. K., Aktoprakoğlu, A., Halkacı, H. S., & Yiğit, O. (2008). Experimental determination of the optimum performance of ejector refrigeration system depending on ejector area ratio. International Journal of Refrigeration, 31(7), 1183-1189.

[14] Huang, B. J., Chang, J. M., Wang, C. P., & Petrenko, V. A. (1999). A 1-D analysis of ejector performance. International journal of refrigeration, 22(5), 354-364.

[15] Huang, B. J., & Chang, J. M. (1999). Empirical correlation for ejector design. International journal of Refrigeration, 22(5), 379-388.

[16] Huang, B. J., Jiang, C. B., & Hu, F. L. (1985). Ejector performance characteristics and design analysis of jet refrigeration system.

[17] Seçkin C. Parametric analysis and comparison of ejector expansion refrigeration cycles with constant area and constant pressure ejectors. J Energy Res Technol – Trans ASME. 2017, 139:4.

[18] Khalil A, Fatouh M, Elgendy E. Ejector design and theoretical study of R134a ejector refrigeration cycle. Int H Refrig. 2011, 34:1684-98.

[19] Cao L, Wang JF, Zhao P, Dai Y. Thermodynamic analysis of a Kalina based combined cooling and power cycle driven by low-grade heat source. Appl Therm Eng. 2017, 111:8-19.

[20] Barkhordarian O, Behbahaninia A, Bahrampoury R. A novel ammonia-water combined power and refrigeration cycle with two-temperature waste heat. Energy Convers Manage. 2017,135:63-73.

[21] Yapıcı, R., & Ersoy, H. K. (2005). Performance characteristics of the ejector refrigeration system based on the constant area ejector flow model. Energy conversion and management, 46(18-19), 3117-3135.

[22] Alexis GK, Karayiannis EK. A solar ejector cooling system using refrigerant R134a in the Athens area. Renew Energy. 2005, 30:1457-69.

[23] Ouzzane M, Aidoun Z. Model development and numerical procedure for detailed ejector analysis and design. Appl Therm Eng. 2003, 23:2337-51.

[24] Huang BJ, Chang JM, Wang CO, Petrenko VA. A 1-D analysis of ejector performance. Int J Refrig. 1999, 22:354-64.

[25] Lear W, Parker G, Sherif S. Analysis of two-phase ejectors with Fabri choking. Proc Inst

Mech Eng C J Mech Eng Sci. 2002,216:607-21.

[26] Shu FH. The physics of astrophysics, vol.2: gas dynamics. Mill Valley: University Science Books. 1991.

[27] Carrillo JAE, Sanchez de La Flor FJ, Salmeron Lissen JM. Thermodynamic comparison of ejector cooling cycles. Ejector characterization by means of entrainment ratio and compression efficiency. Int J Refrig. 2017, 74:369-82.